AD A124 421 THE FABRICATION OF DOUBLE HETEROSTRUCTURE ALUMINUM GALLIUM ARSENIDE/GALLI..(U) ILLINOIS UNIV AT URBANA COORDINATED SCIENCE LAB T J DRUMMOND JUL 82 R-951 1/1

UNCLASSIFIED N000014-79-C-0424 F/G 20/12 NL

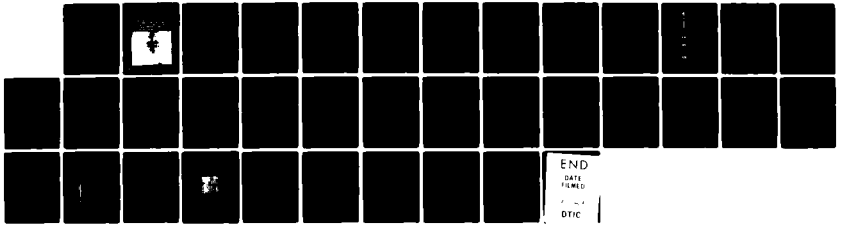

END

DATE FILMED

DTIC

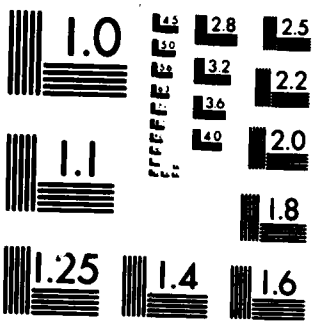

REPORT R-951 JULY, 1982 UILU-ENG 82-2217

CSL COORDINATED SCIENCE LABORATORY

(12)

THE FABRICATION OF DOUBLE HETEROSTRUCTURE ALUMINUM GALLIUM ARSENIDE/ GALLIUM ARSENIDE LASERS BY MOLECULAR BEAM EPITAXY

UNIVERSITY OF ILLINOIS AT URBANA-CHAMPAIGN

UNCLASSIFIED

SECURITY CLASSIFICATION OF THIS PAGE (When Data Entered)

REPORT DOCUMENTATION PAGE	READ INSTRUCTIONS BEFORE COMPLETING FORM
1. REPORT NUMBER	2. GOVT ACCESSION NO. AD-A124421	3. RECIPIENT'S CATALOG NUMBER
4. TITLE (and Subtitle) THE FABRICATION OF DOUBLE HETEROSTRUCTURE ALUMINUM GALLIUM ARSENIDE/GALLIUM ARSENIDE LASERS BY MOLECULAR BEAM EPITAXY	5. TYPE OF REPORT & PERIOD COVERED 6. PERFORMING ORG. REPORT NUMBER R-951 UILU-ENG 82-2217
7. AUTHOR(s) Timothy J. Drummond	8. CONTRACT OR GRANT NUMBER(s) N00014-79-C-0424
9. PERFORMING ORGANIZATION NAME AND ADDRESS University of Illinois Coordinated Science Laboratory Urbana, IL 61801	10. PROGRAM ELEMENT, PROJECT, TASK AREA & WORK UNIT NUMBERS
11. CONTROLLING OFFICE NAME AND ADDRESS Joint Services Electronics Program Research Triangle Park, NC 27709	12. REPORT DATE 1982 13. NUMBER OF PAGES 32
14. MONITORING AGENCY NAME & ADDRESS (if different from Controlling Office)	15. SECURITY CLASS. (of this report) Unclassified 15a. DECLASSIFICATION/DOWNGRADING SCHEDULE

16. DISTRIBUTION STATEMENT (of this Report)

Approved for public release, distribution unlimited

17. DISTRIBUTION STATEMENT (of the abstract entered in Block 20, if different from Report)

18. SUPPLEMENTARY NOTES

19. KEY WORDS (Continue on reverse side if necessary and identify by block number)

Double Heterostructure Laser
Molecular Beam Epitaxy
$Al_xGa_{1-x}As/GaAs$

20. ABSTRACT (Continue on reverse side if necessary and identify by block number)

GaAs-$Al_xGa_{1-x}As$ Double-Heterostructure (DH) lasers with current-threshold densities comparable to similar geometry DH lasers prepared by liquid phase epitaxy have been successfully prepared in a commercial molecular beam epitaxy (MBE) system for the first time. For a structure with a 2300 Å thick active layer, the threshold current density at room temperature was 1.4 KA/cm^2 with a differential quantum efficiency of 45%.

DD FORM 1 JAN 73 1473

SECURITY CLASSIFICATION OF THIS PAGE (When Data Entered)

THE FABRICATION OF DOUBLE HETEROSTRUCTURE ALUMINUM GALLIUM ARSENIDE/GALLIUM ARSENIDE LASERS BY MOLECULAR BEAM EPITAXY

BY

TIMOTHY JAMES DRUMMOND

B.S., Michigan State University, 1979

THESIS

Submitted in partial fulfillment of the requirements
for the degree of Master of Science in Electrical Engineering
in the Graduate College of the
University of Illinois at Urbana-Champaign, 1982

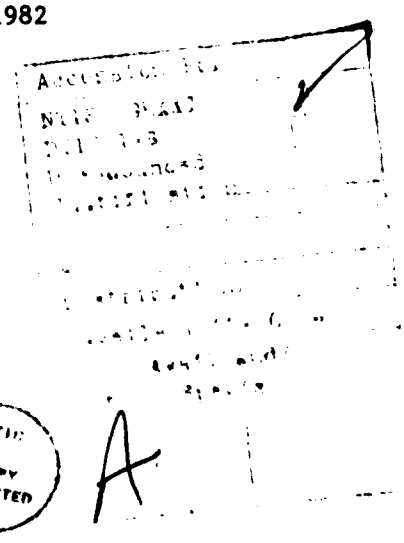

Urbana, Illinois

ACKNOWLEDGEMENTS

The author is greatly indebted to his advisor, Hadis Morkoç, for the large amount of time and patience invested in teaching him the art of molecular beam epitaxy. The aid of Dr. A. Y. Cho of Bell Laboratories was invaluable. He was responsible for the device fabrication and testing of the lasers after they were grown. His continuing interest and support is deeply appreciated. Special thanks are extended to his present colleagues, Bill Kopp and Russ Fischer, who took over much of the work load during the writing of this thesis. The author would like to thank Professor K. Hess for his encouragement and many interesting and valuable discussions. Also deserving much credit is Professor L. J. Giacoletto of Michigan State University whose initial interest and efforts led the author to graduate work in the field of semiconductors.

The many members of the staff of the Coordinated Science Laboratory provided valuable support for this project. Thanks are extended to Lyle Bandy, George Bouck, Bill Beaulin, Jack Gladin, Bob MacFarlane and Clay Lofton for their assistance and to Mary Foster and Susan Brennecke for their help in the typing and preparation of this thesis.

Finally the author would like to thank Aaron and Ruth DeJule for their friendship and to his parents, Tom and Nancy, for their continual support, encouragement and love.

TABLE OF CONTENTS

I. INTRODUCTION

Today there exists a need to be able to process increasing amounts of data at rates beyond the capabilities of existing purely electrical networks. To meet this need, networks which transmit data via an optical carrier rather than an electrical one are being developed. A necessary component of an optical network is a small, easily modulated source of coherent light. The only such source available is a laser diode.

The first laser diode to operate continuously at room temperature was a double heterostructure (DH) (Al,Ga)As/GaAs laser prepared by liquid phase epitaxy (LPE).[1] Much effort was subsequently devoted to reproducing those results by molecular beam epitaxy (MBE). MBE offers several advantages over LPE, such as control of composition and impurity profiles to atomic dimensions. Layers can be grown on larger substrates and with a high degree of uniformity and reproducibility that is not possible with LPE. Despite these advantages, it was six years after the first continuous room temperature operation of an (Al,Ga)As/GaAs DH laser that a similar laser prepared by MBE was reported.[2] The first MBE lasers typically had threshold current densities, J_{th}, about twice as large as similarly designed LPE lasers. Another three years passed before the art of MBE advanced to the point where it became possible to achieve laser performance equal to the LPE lasers.[3]

The presence of non-radiative recombination centers in the bulk (Al,Ga)As layers was shown to make a significant contribution to the high threshold current densities in MBE lasers.[4] The source of these centers is believed to be oxygen, which is readily incorporated at a growing (Al,Ga)As surface because of the high reactivity between oxygen and aluminum. Oxygen is present in the growth chamber as CO, H_2O and O_2. To overcome this problem, MBE systems were redesigned to have growth chambers which could be isolated

from a sample introduction chamber and kept in an ultra high vacuum (UHV) at all times. A liquid nitrogen cryoshroud was incorporated to freeze out any remaining traces of condensible atmospheric contaminants. These, and other, design improvements made it possible to prepare laser quality material with MBE.

To date, however, the only lasers to be prepared by MBE have been fabricated from lasers grown in custom built systems. To demonstrate the feasibility of moving MBE grown lasers from a research to a production oriented basis, this thesis describes the preparation of DH (Al,Ga)As/GaAs laser structures in a commercially available system. Broad area lasers with threshold current densities as low as 1.4×10^3 A/cm^2 and a differential quantum efficiency of 45% when operated CW at room temperature have been prepared. These values compare favorably with similar commercial devices currently available for use in optical communication systems.

II. MOLECULAR BEAM EPITAXY

Molecular beam epitaxy (MBE) is an ultra-high-vacuum deposition technique applied primarily to the growth of compound semiconductor layers.[5,6,7] Growth is achieved by impinging thermal beams of semiconductor and impurity elements upon a heated substrate. III-V compound semiconductors, such as GaAs, can easily be grown by maintaining a stoichiometric excess of the column V element. In this case, the growth rate will be determined by the arrival rate of the column III element or elements in the case of ternary compounds, such as (Al,Ga)As. Similarly, the doping levels can be controlled by adjusting the flux of the appropriate dopants. Abrupt changes in composition and doping profile can be achieved by using mechanical shutters in front of sources to control the initiation and cessation of any molecular beam. This is possible because the growth rates are on the order of two angstroms per second and thus the shutters can be actuated in much less time than it takes to grow a single monolayer. Sharp profiles are typically maintained at the low growth temperatures (450 to 700°C) used during MBE growth. Both liquid phase and vapor phase epitaxy require substrate temperatures in excess of 800°C where diffusion of impurities during growth can be significant.

The MBE system at the University of Illinois is a commercially available research-oriented machine. This system is composed of three separate vacuum chambers, as illustrated in Figure 1. The chambers can be isolated from one another by gate valves. Facing the front of the system, the analysis chamber is on the right hand side and is equipped with an Auger electron spectrometer. The growth chamber is on the left hand side and is equipped with a Quadrupole Mass Analyser (QMA) and High Energy Electron Diffractometer (HEED). A small sample introduction chamber is located in the

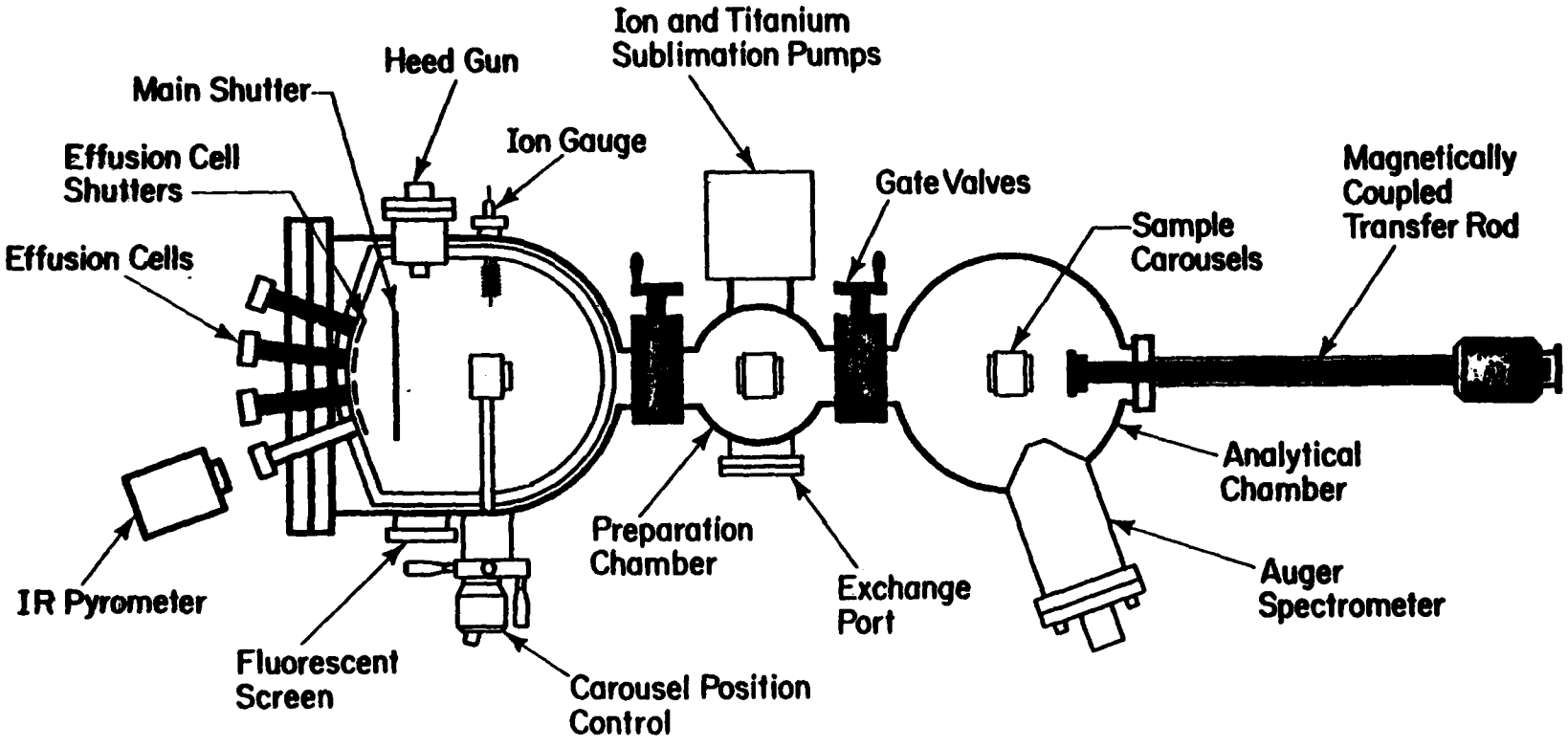

Molecular Beam Epitaxy System

Figure 1. A schematic view of the system as seen from above.

center. The introduction chamber can be brought up to atmospheric pressure independently of the growth chamber and analysis chamber. This allows samples to be loaded into the system without exposing the other chambers to atmospheric contaminants such as oxygen, water vapor and carbon monoxide. The small size of the chamber allows for rapid pumping down to a base pressure of 1×10^{-8} torr (1.3×10^{-6} pascal).

After the base pressure has been achieved, the gate valves can be opened to allow samples to be transferred from one chamber to another. This is accomplished by means of a magnetically coupled transfer rod possessing translational and rotational freedom. When not in use, the transfer rod resides entirely in a steel sleeve extending outward from the analytical chamber. The magnetic coupling enables travel along and rotation about the long axis of the system. The primary advantage of the magnetic coupling is that it maintains the vacuum in the system without the complexity of a bellows mechanism.

The growth chamber is approximately hemispherical and a detailed schematic, as viewed from above, appears in Figure 2. Samples are mounted on a carousel located in the center of the growth chamber. The carousel possesses several degrees of freedom by utilizing several mechanical bellows-type feedthroughs. The sample can be rotated in the plane which bisects the growth chamber. It can be positioned in an x-y-z frame about the center of the chamber and it can be rotated about an axis perpendicular to the plane of the substrate. During the transfer process, the carousel is positioned to face the introduction chamber. Once the sample block is mounted on the carousel, the transfer rod is withdrawn, the gate valve is closed and the sample is rotated to face the opposite wall of the growth chamber. Mounted in this wall are two tiers of effusion cells.

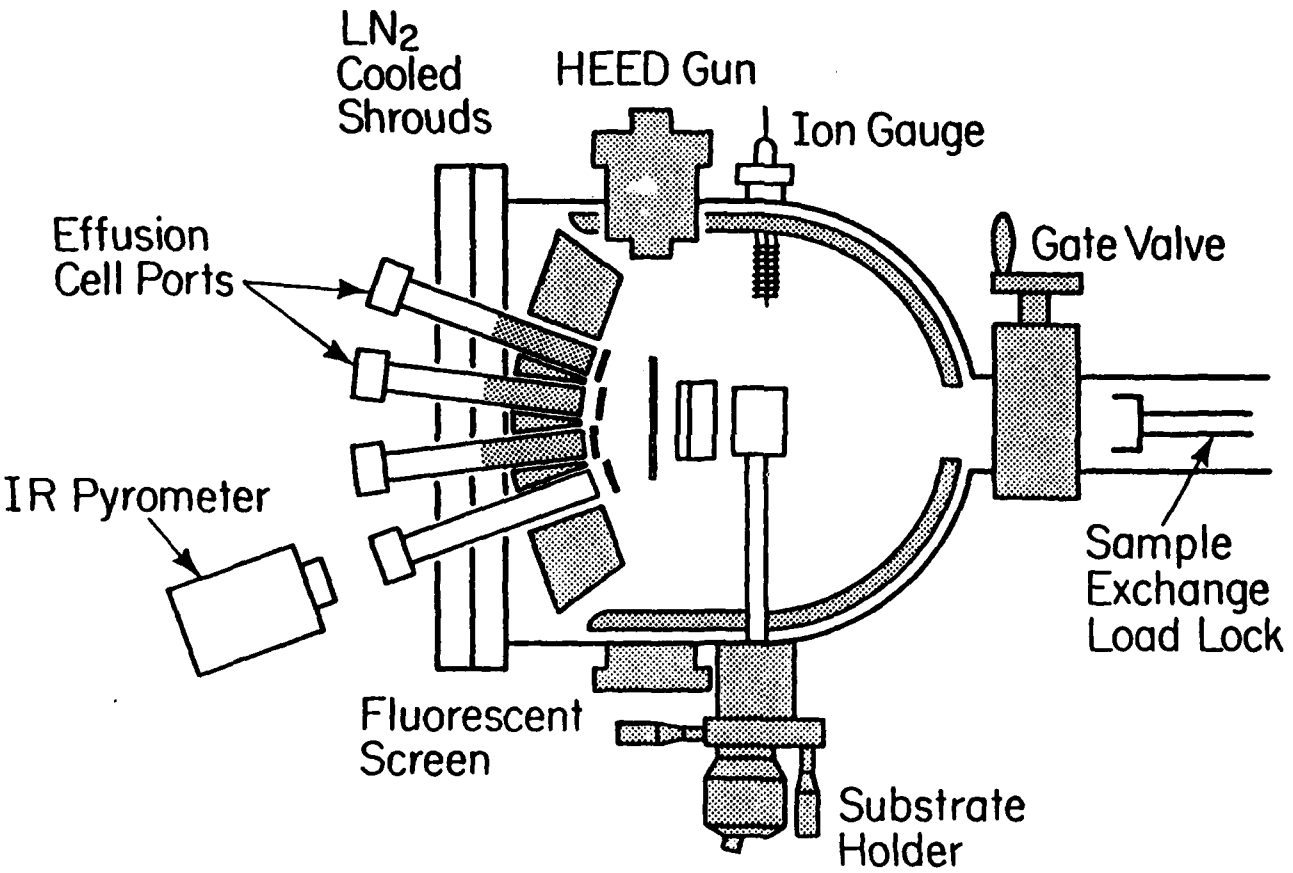

Figure 2. A schematic view of the growth chamber as seen from above.

The effusion cells are ovens in which the semiconductor and dopant source charges are vaporized. They are positioned with the upper tier 5^{o} below horizontal and the lower tier 21.5^{o} below horizontal. In addition, they are positioned as close to horizontal as is practical to prevent the cells from being contaminated by material flaking off the walls of the growth chamber and falling into the cells. This is a significant problem because a large fraction of the molecular beams are deposited on the walls of the growth chamber.

The effusion cells are made of high purity pyrolytic boron nitride crucibles mounted in resistance heated furnaces. The temperature of the cell is measured by a tungsten/rhenium thermocouple butted into a depression in the bottom of the crucible. The thermocouple provides an input signal to a regulator controlling the power delivered to the furnace. The temperature can be regulated to better than one degree Celsius in this manner. Each furnace is thermally isolated by a liquid nitrogen cryoshroud which continues around to envelope the entire growth chamber. The cryoshroud serves the second function of ensuring that the excess flux from the effusion cells is adsorbed on the walls of the shroud during a growth. If this were not the case, excess dopants would build up in the growth chamber ambient, causing doping to persist after the dopant flux was terminated.

Other features of the growth chamber include a main shutter, an ion gauge, a HEED system and a QMA. The main shutter is designed to block the flux paths of all of the effusion cells simultaneously and is used to initiate and terminate the growth. To initiate the growth, the individual shutters for the requisite elements are opened. The main shutter is then opened, which ensures that the arrival of beams at the substrate surface is synchronized. Similarly, to terminate the growth, the main shutter is employed to

synchronously terminate the beams.

A nude Bayard-Alpert ion gauge located behind and offset to one side of the sample as it faces the effusion cells. The primary function of the ion gauge is to monitor the As flux. To obtain high quality GaAs, an excess of As must be maintained, and its partial pressure in the growth chamber must constitute at least 75% of the total pressure. This allows the As flux to be maintained at the desired level by simply maintaining the pressure in the growth chamber at a predetermined level.

The QMA is located immediately above the sample in the growth chamber and is used to make accurate determinations of the relative flux ratios during growth. The QMA can be used to determine the As/Ga ratio necessary to optimize the growth of GaAs. It can also be used to determine the AlAs mole fraction when growing (Al,Ga)As since the mole fraction is proportional to the Al/Ga flux ratio. In some respects, however, the QMA is of limited use because it tends to become saturated if left in the growth chamber for several growths. Furthermore, once the conditions are known to obtain a given flux intensity, they are extremely reproducible over long periods of time and the use of the QMA may not be required at all times.

HEED is employed to observe the surface structure of the crystal prior to and during growth. Prior to growth, it can determine whether the surface oxide layer is desorbed by the thermal outgassing of the crystal. Subsequently, it can be used to determine if the crystal growth is single crystalline. If a compositional change is made during the growth which produces an interface at which a lattice mismatch can occur, the transition can be monitored to ensure that single crystal growth is maintained.

After a crystal is grown, in-situ analysis of the film can be performed in the analysis chamber. The analysis chamber has a centrally located sample carousel which is used to position the sample in front of the Auger electron spectrometer. The carousel sample mount incorporates a resistive heating element which allows studies of the surface at temperatures above room temperature.

Because an oxide layer cannot grow in the vacuum system, an in-situ Auger spectrometer also facilitates studies of the effect of annealing on thin films. A film can be grown in the growth chamber, transferred to the analysis chamber, and an Auger spectrum taken. Subsequent annealing is done after the sample is returned to the growth chamber so that the annealing can be done under As rich conditions. This is necessary because GaAs decomposes at high temperatures (about 550^{o}C) by the preferential loss of As from the surface.

III. SUBSTRATE PREPARATION AND EPITAXY

The substrates used for MBE are typically (001) oriented GaAs wafers, fifteen to thirty mils thick. Substrates intended for field effect transitors are Cr doped and semi-insulating. Substrates for lasers or other optical applications are Si doped and n-type. Si doped substrates are chosen for optical applications because they can be produced with very low etch pit densities. After the appropriate substrate is selected, the first step in preparing it for epitaxy is to degrease it in a series of organic solvents. Substrates are cleaned, in order, in boiling trichloroethane, trichloroethane, acetone, methanol and deionized water. If the wafer is initially unpolished, a mirror surface is obtained by polishing the wafer on a pellon cloth soaked in a weak solution of bromine-methanol.

Immediately before the substrate is loaded into the system, it is cleaved into square samples two and a half centimeters on a side. The (001) wafers can be easily cleaved along the (110) planes which are mutually perpendicular as well as perpendicular to the (001) direction. After cleaving, the substrate is placed in a sulfuric acid/hydrogen peroxide/deionized water etch which is intended to remove the top ten to twenty microns from the surface of the wafer. The substrate is subsequently rinsed in deionized water and then placed in hydrochloric acid for approximately one minute to passivate the surface against oxidation. After a final rinse in deionized water, the substrate is dried with a dry nitrogen jet and mounted on a molybdenum sample block.

The introduction chamber is isolated from the growth and analysis chambers and backfilled with dry nitrogen. The backfilling minimizes contamination of the introduction chamber with oxygen and water vapor while the chamber is open. Access to the introduction chamber is through a six inch

vacuum flange. The flange is removed, samples which have epilayers grown on them are removed, and the blocks with new substrates are loaded. The six inch flange is immediately replaced and the pump-down cycle is initiated. The pumping proceeds in three stages. A mechanical pump is used down to a pressure of ninety torr (1.2×10^4 pascal) at which point a bank of sorbtion pumps used in series lowers the pressure to less than 1×10^{-3} torr (1.3 pascal). The ion pump is then turned on, which pumps the introduction chamber to a pressure of 10^{-8} torr (1.3×10^{-6} pascal) in four hours. A pressure in the low 10^{-9} torr (1.3×10^{-7} pascal) range can be achieved in twenty-four hours. If faster pumping speeds are required, the titanium sublimation pump can be used.

Shortly after the ion pumps are turned on and the pressure in the introduction chamber is about 1×10^{-6} torr (1.3×10^{-4} pascal), the substrates are thermally outgassed to remove surface contaminants and oxides. After outgassing, the substrates are left in the introduction chamber until the pressure reaches 1×10^{-8} torr (1.3×10^{-6} pascal). At this point, the pressure is typically less than that in the growth chamber and the substrate can be transferred to the growth chamber with a minimum of cross-contamination of residual atmospheric gases remaining in the preparation chamber.

With the substrate in the growth chamber, the carousel is adjusted so that the center of the substrate is located at the focal point of the effusion cells. The liquid nitrogen cryoshroud is filled and the pressure in the growth chamber drops to mid 10^{-10} torr (1.3×10^{-8} pascal) range. With the shroud cold, the effusion cells are heated. Typically, the effusion cells are outgassed by briefly raising the temperature of each cell to a point ten to fifty degrees above the temperatures required for epitaxy. After outgassing the effusion cells, the substrate is heated and outgassed at a temperature

between 615 and 630°C. Experiments with HEED and Auger electron spectroscopy indicate that the amorphous oxide layer on the crystal surface desorbs at 580°C (Ref. 8). The temperature is immediately reduced after it reaches the outgas temperature which is measured by an infrared pyrometer focused on the crystal surface. As the temperature approaches the growth temperature, the main shutter is closed in preparation to starting the growth.

With the main shutter closed, the individual shutters covering the effusion cells are opened. Growth is then initiated by opening the main shutter. During the growth, dopants can be turned on and off by opening and closing the appropriate shutters. The University of Illnois' system employs two As cells, a Ga cell and an Al cell for III-V element sources. N-type dopants are Si and Sn,[9,10] and the p-type dopant used is Be.[11,12] The individual shutters can be actuated manually or by an automatic shutter controller.[13] Due to low growth rates, graded doping and compositional profiles are possible. This is achieved by manually varying the set temperature of the effusion cell temperature controller. The automatic timer has four channels which can be set to open and close shutters in any predetermined sequence. To grow multilayer structures such as superlattices, the timer can be set to cycle through the sequence up to 9,999 times.

The impurity doping levels in the epilayer are determined by the growth rate of the crystal and the flux density of incident impurity atoms. The beam fluxes are exponentially dependent on temperature over the ranges of interest. The exact dependence must be determined empirically for each dopant because the flux depends on the design of the pyrolytic boron nitride crucible and the amount and type of the source material in it. Once the relationship had been determined, it could be represented in a readily usable form as a straight line on a semilog graph with the doping level normalized to a one micron per

hour growth rate.

Termination of the growth is accomplished simply by closing the main shutter and turning off the power to the substrate heater. In this fashion the beams are simultaneously interrupted and the surface of the crystal is effectively frozen. The temperature of the mounting block is observed to drop over two hundred degrees in less than a minute as measured by a thermocouple butted against the back face of the block.

IV. LASERS: DISCUSSION

The laser diode is becoming an important component in modern communication systems. The advantages of the laser diode are its small size, the capability of easily modulating the light output with an electrical signal and its future potential for integrated optical circuits.[14] Presently, most laser diodes are fabricated as discrete devices and the performance of the laser is dependent upon both the quality of the semiconductor material from which it is made and the device "geometry" of the laser. The first laser diodes were prepared by liquid phase epitaxy (LPE) and lased only when pulsed at cryogenic temperaures ($\leq$ 78 K). Improvements in the design of the laser structure led to CW operation at room temperature. Research is now directed toward lowering the lasing threshold current density and tailoring the wavelength of the output radiation for specific applications. LPE is limited as a growth technique because it can utilize only a small substrate area, as well as having layer thickness control down to only about 100 Å. MBE can be used to grow on much larger substrates and layers can be grown with monolayer accuracy (2 - 3 Å). Despite the inherent advantages of MBE, only in the past few years has it been possible to obtain lasers comparable to and better than similar LPE grown lasers.

Semiconductor lasers must be made of direct bandgap materials. In a semiconductor laser, photons are generated by the direct recombination of electrons in the conduction band with holes in the valence band. In an indirect semiconductor recombination must proceed via a two step process involving both a photon and a phonon to conserve momentum. Consequently, the probability for recombination in an indirect semiconductor is small enough that competing non-radiative recombination processes make it impossible to generate enough photons to achieve lasing. Lasing has been observed in many

direct gap compound semiconductors. The first laser diode was made of GaAs and today most laser structures incorporate a GaAs active region clad by (Al,Ga)As confining layers in a double heterostructure configuration.

To understand the advantages of MBE and the difficulties which had to be overcome, an understanding of how lasing is accomplished in a semiconductor is necessary. Lasing implies that the output radiation is coherent and that the gain at least equals the losses. This will occur if an inverted electron population can be maintained in a low loss Fabry-Perot cavity. An inverted electron population is illustrated in Figure 3 for a semiconductor at 0 K. Electron-hole recombination will produce photons of frequency, ν, such that $h\nu \sim E_g$ where h is the reduced Planck's constant and E_g is the band gap energy of the semiconductor. If the quasi-Fermi levels for electrons and holes, F_e and F_h, are such that $F_e - F_h \geq 2$ kT then the stimulated emission will dominate over spontaneous emission of photons.[15] Photons emitted by stimulated emission are in phase with stimulating photons. In a semiconductor, recombination can take place between several different pairs of energy levels, hence the output radiation is not monochromatic. The purpose of the Fabry-Perot cavity is to select a single frequency and amplify it to the point where the gain exceeds the losses and lasing occurs.

A simple Fabry-Perot cavity, such as that employed in the first laser diodes, is depicted in Figure 4. It is a small rectangular slab containing the junction plane of the diode. The ends perpendicular to the long axis must be parallel and be partially reflecting mirrors. The ends perpendicular to the short axis may be rough or mirrors. When the length of the cavity is equal to an integral number of half wavelengths, a standing wave is set up in the cavity. If the sides parallel to the long axis are mirrors, then standing waves involving reflections from all four walls are possible. Lasing occurs

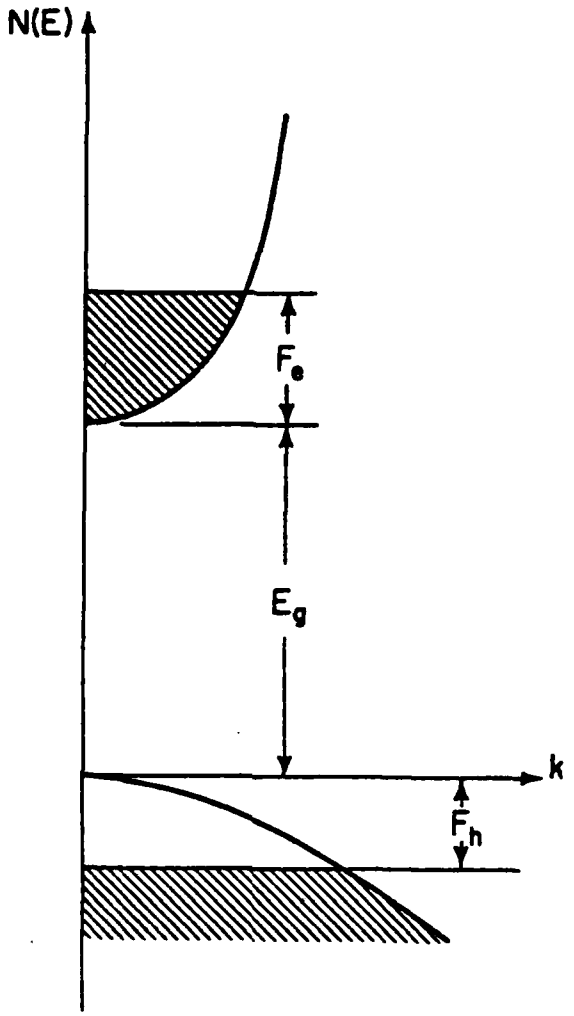

Figure 3. A band diagram of an inverted electron population at 0 K.

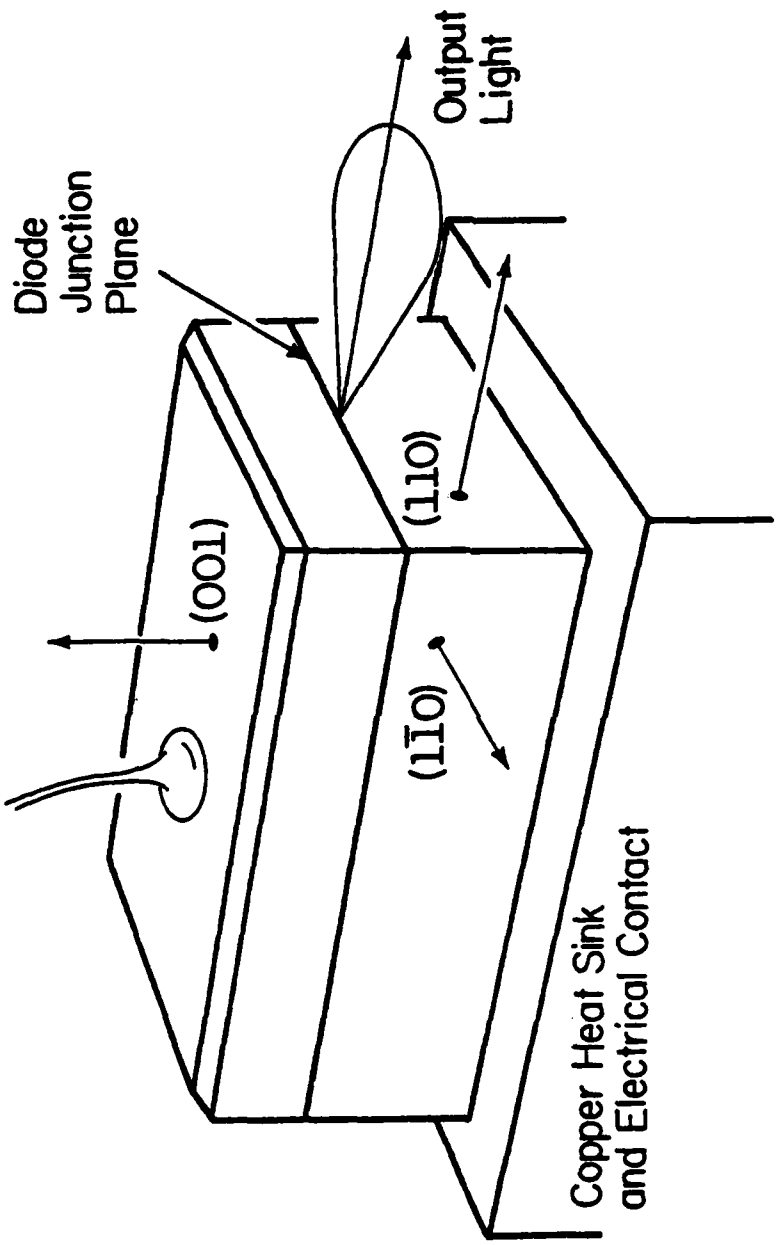

Figure 4. A schematic diagram of the physical structure of a diode laser.

at wavelengths for which standing wave modes in the cavity exist.

Given an appropriate Fabry-Perot cavity, it is also necessary to achieve net gain in the cavity in the coherent light generated. If light with an intensity of I_o is emitted from a point in the center of a cavity of length ℓ it must travel to one end of the cavity where a fraction R_1 is reflected back into the cavity. The light then travels to the other end of the cavity where a fraction R_2 is reflected back to the point of origin. For lasing to occur, the total gain must at least equal the losses, which implies that the intensity, I, of the light returning to the point it was emitted from must at least equal I_o. In p-n junction laser diodes where the population inversion is maintained by the forward current, the threshold current density necessary to achieve the above condition can be shown to be

$$J_{th} = \frac{\alpha}{\beta} + \frac{1}{2\ell\beta} \ell n \left(\frac{1}{R_1 R_2}\right)$$

where α is the loss coefficient per unit length and β is the gain factor in A/cm.[14] Using this equation, the basic requirements of fabricating a Fabry-Perot cavity can be discussed.

An optical cavity with mirror ends is easy to fabricate if the p-n junction is grown on a (100) oriented GaAs wafer. By cleaving along the (110) planes, a rectangular cavity with plane parallel edges can be formed. Due to the high index of refraction of GaAs, the reflectivity of the GaAs/air interface is approximately 0.32. Once the cavity is formed, the next most important factor in determining the threshold current density is the loss coefficient . The electron population inversion is maintained only near the junction. Electrons are free to diffuse away from the junction and there is very little optical confinement so that much of the light is radiated into the

bulk material, away from the junction and reabsorbed. Further losses arise if there is a significant trap concentration giving rise to non-radiative recombination. The first two loss mechanisms can be reduced by placing the thin "active" layer of GaAs between confining layers of (Al,Ga)As with the p-n junction being at one of the heterointerfaces. (Al,Ga)As has a larger bandgap and refractive index than GaAs so that the (Al,Ga)As layers confine both electrons and light in the GaAs layer.

Further carrier confinement is achieved in the "proton bombarded stripe geometry" laser.[16] To fabricate a proton bombarded stripe geometry laser, a small rectangle is cleaved from a wafer with a DH laser structure. A stripe of gold is deposited along the lasing axis. The surface is then bombarded with protons of energy sufficient to disorder the crystal down to but not including the active GaAs layer. The gold stripe acts as a mask and the crystal beneath it is undamaged. The gold stripe is then used as the contact to the surface side of the diode and current is constrained to flow vertically under the stripe. If the bombardment damage extends into the active layer, nonradiative recombination at the damage/no damage interface increases the threshold current density, especially for narrow stripes.[17] The purpose of the stripe geometry is to reduce the number of higher order transverse modes and consequently narrower stripe widths are desirable.

Given comparable stripe geometry lasers fabricated by LPE and MBE, one would expect better performance from MBE grown wafers. Sn doped GaAs, which is commonly used as the active region in DH lasers as characterized by photoluminescence properties, can be grown with better quality by MBE than LPE.[18] Also, MBE has the advantage of much better control over the layer thickness and uniformity. The difficulty encountered in achieving DH lasers is the presence of deep level traps in (Al,Ga)As layers.[4] Aluminum is highly

reactive and residual O_2, CO and H_2O in the MBE growth chamber will lead to traps due to the incorporation of oxygen. The presence of these recombination centers in bulk (Al,Ga)As can account for the observed poor performance of DH lasers prior to 1978. Improved system design and the discovery that higher growth temperatures significantly reduce deep level trap concentrations brought forth MBE grown lasers with performance superior to LPE grown lasers.

V. LASERS: RESULTS AND SUMMARY

Both broad area and stripe geometry lasers were fabricated from double heterostructures grown at the University of Illinois. Figure 5 is a scanning electron micrograph of the (110) cleaved cross-section of a DH laser structure and Figure 6 shows schematically the time-temperature sequence used in growing this structure. The solid lines indicate effusion cell temperatures when the cells are open and broken lines indicate temperature of the cells when shutters are closed. All layers were grown on Si doped GaAs substrates, the preparation of which has already been described. The GaAs growth rate was 0.77 μm/hr and the Al flux was adjusted to obtain a 30% AlAs mole fraction. The substrate temperature was held at 600°C for the growth of n-type layers and 625°C for the active layer and p-type layers.

The layer thicknesses are delineated in Figure 5, except for the initial GaAs buffer layer which is grown to avoid any effects due to inferior quality substrates. The only important dimension in the structure is the active layer thickness which is 2,300 Å. The purpose of the surface GaAs layer is to facilitate the formation of an ohmic contact to the diode.

The broad area lasers were fabricated with a cavity length of 380 μm and a cross-section area of about 5×10^{-4} cm^2. Current densities as low as 1.4×10^3 A/cm^2 were obtained. Figure 7 shows the current-voltage characteristics of a broad area laser. The horizontal scale for forward bias is 0.5 V/div and that for reverse bias is 2 V/div. The vertical current scale is 0.5 mA/div in both cases. Figure 8 is a typical light-current characteristic for a laser under pulsed operation. The sharp turn-on indicates a differential quantum efficiency of approximately 45%. Proton bombarded stripe geometry lasers with 5 μm x 350 μm stripes were also fabricated. A threshold current density of 8.5×10^3 A/cm^2 was obtained. A

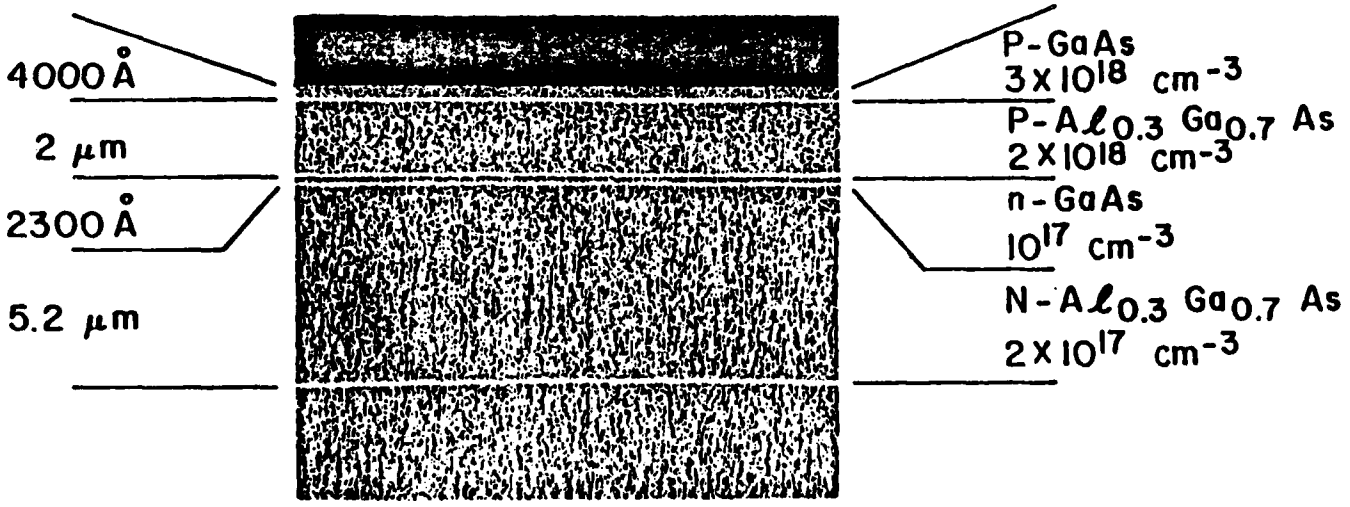

Figure 5. A scanning electron micrograph of a DH laser grown at the University of Illinois.

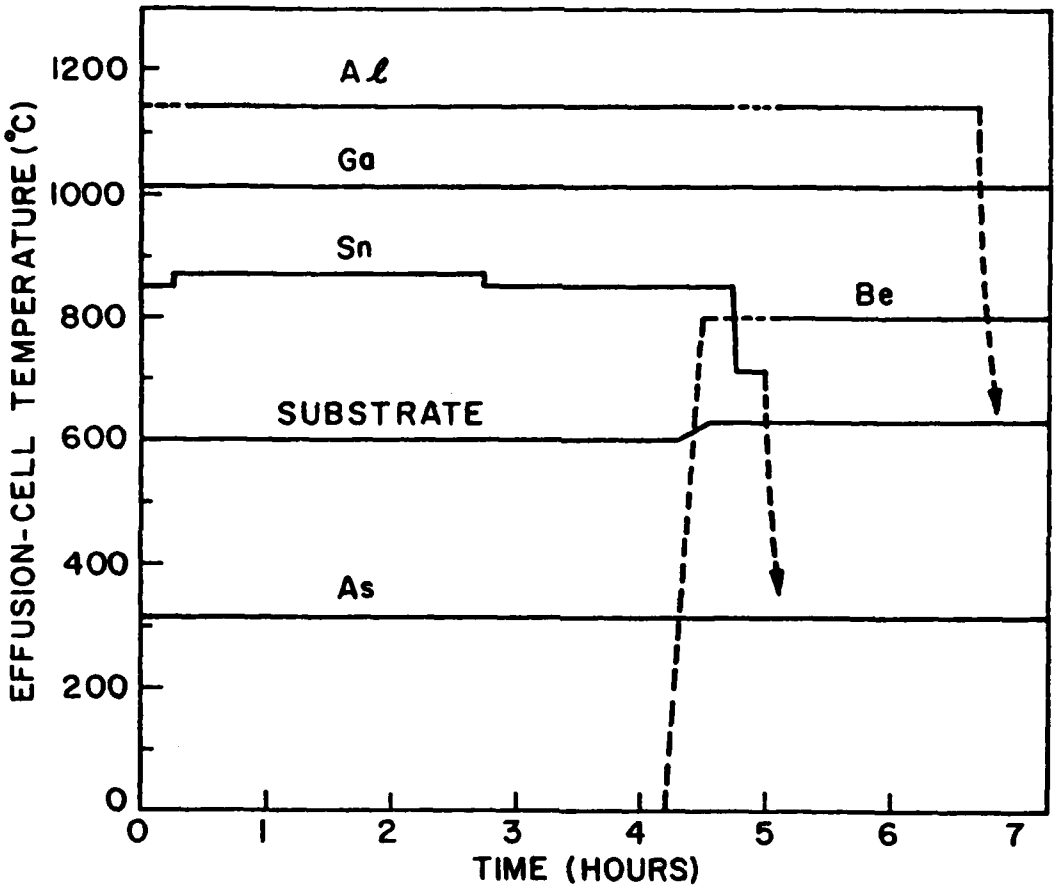

Figure 6. Temperature-time cycle used to grow the GaAs-$Al_xGa_{1-x}As$ DH lasers. Solid lines indicate open shutters; dashed lines indicate closed shutters.

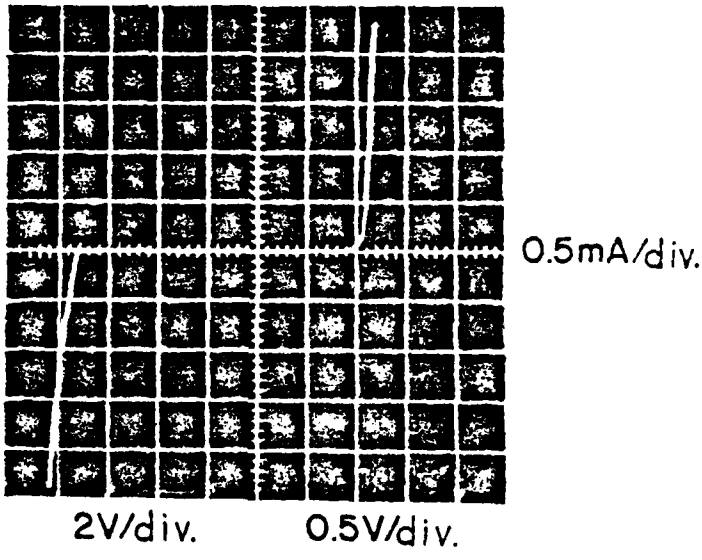

Figure 7. A typical current-voltage characteristic of the broad area laser.

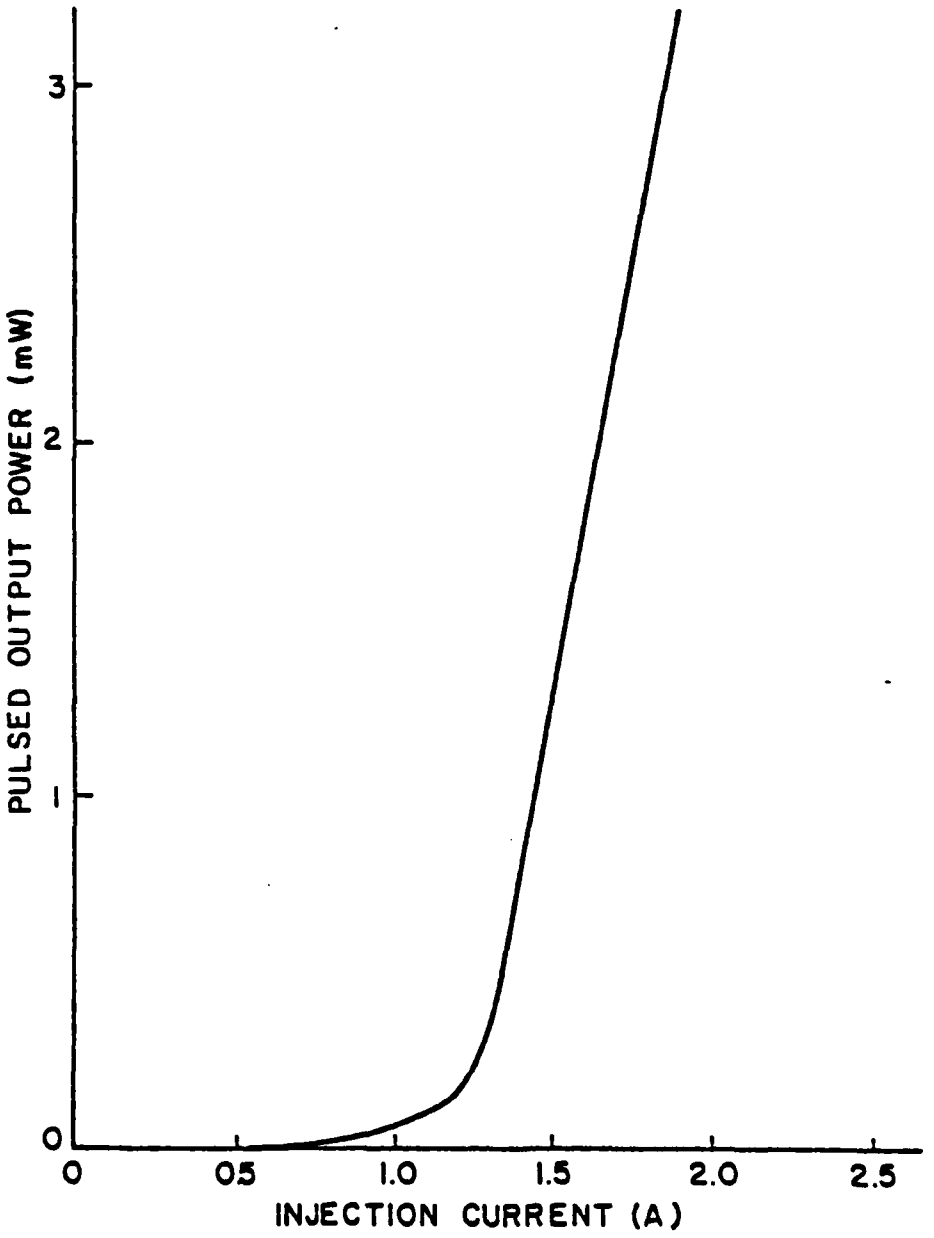

Figure 8. Typical light-current characteristics for a DH laser with a cross-sectional area of 140 x 380 μm under pulsed operation.

typical current density value for similar lasers prepared elsewhere by MBE is 6.5×10^3 A/cm^2 (Ref. 19). The light-current characteristics for a typical stripe geometry laser being run CW at 300 K are shown in Figure 9. Curves (A) are the light-current characteristic at each mirror, curves (B) and (C) are first and second derivatives, respectively, of the voltage-current characteristic.

In summary, both broad area and proton bombarded stripe geometry lasers have been fabricated from layers grown in a commercially available molecular beam epitaxy system. The low threshold current densities exhibited by these lasers demonstrate that MBE is a technology which can successfully compete with LPE in producing state-of-the-art optical devices. MBE has the advantage of being the more efficient technology in terms of yield per substrate and reproducibility.

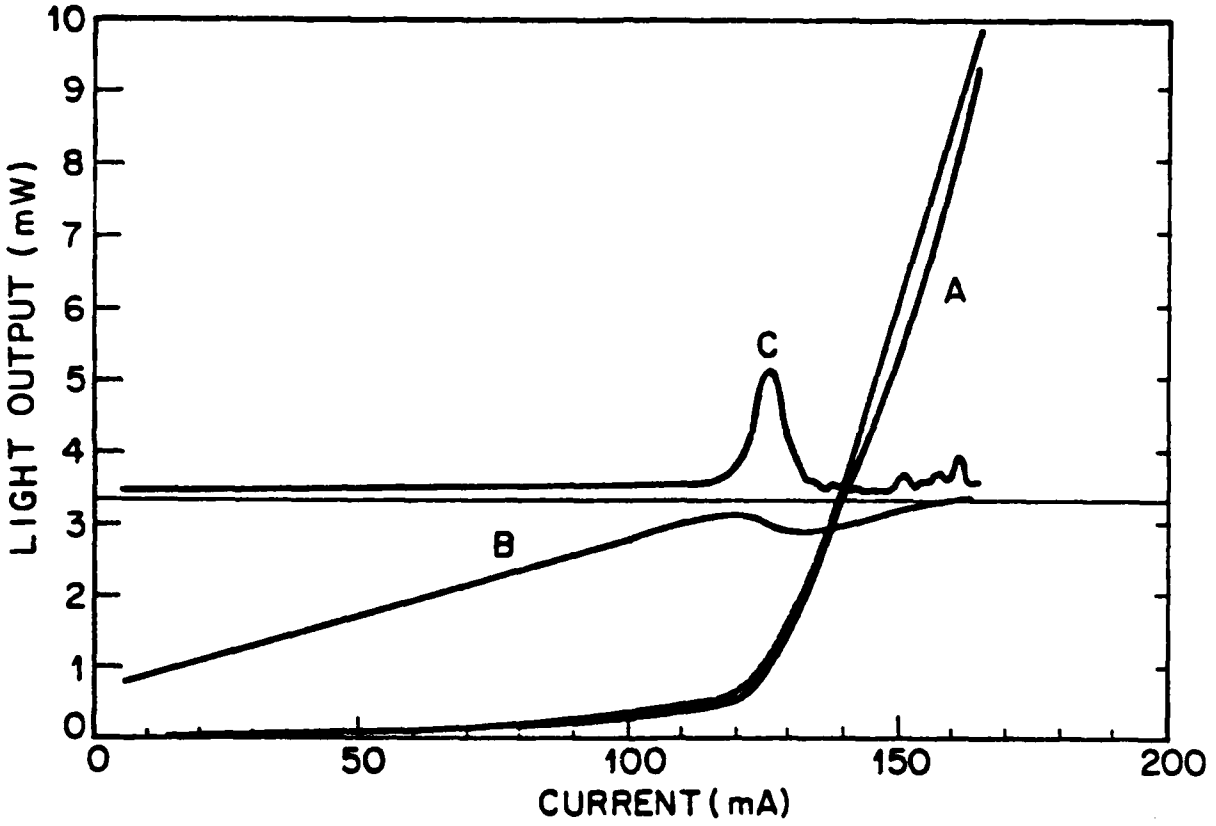

Figure 9. (A) Light current characteristics from each mirror,
(B) the first derivative and
(C) the second derivative of the voltage with respect to current versus current for a typical stripe geometry laser operating CW at room temperature.

REFERENCES

1. I. Hayashi, M. B. Panish, P. W. Foy and S. Sumski, "Junction Lasers Which Operate Continuously at Room Temperature," Appl. Phys. Lett., 17, 109, 1970.

2. A. Y. Cho, R. W. Dixon, H. C. Casey and R. L. Hartman, "Continuous Room-Temperature Operation of GaAs-$Al_xGa_{1-x}As$ Double Heterostructure Lasers Prepared by Molecular Beam Epitaxy," Appl. Phys. Lett., 28, 501, 1976.

3. W. T. Tsang, "Low-Current-Threshold and High-Lasing Uniformity GaAs-$Al_xGa_{1-x}As$ Double-Heterostructure Lasers Grown by Molecular Beam Epitaxy," Appl. Phys. Lett., 34, 473, 1979.

4. W. T. Tsang, "The Influence of Bulk Nonradiative Recombination in the Wide Band-Gap Regions of Molecular Beam Epitaxially Grown GaAs-$Al_xGa_{1-x}As$ DH Lasers," Appl. Phys. Lett., 33, 245, 1978.

5. A. Y. Cho and J. R. Arthur, "Molecular Beam Epitaxy," Progress in Solid State Chemistry (Pergamon Press), 10, 157, 1975.

6. M. B. Panish, "Molecular Beam Epitaxy," Science, 208, 916, 1980.

7. T. G. O'Neill, "Production Oriented MBE Systems," Semicon. International, 3, 57, 1980.

8. T. J. Drummond, H. Morkoç and A. Y. Cho, "Molecular Beam Epitaxy Growth of (Al,Ga)As/GaAs Heterostructures," to be published in J. Crystal Growth, 1981.

9. A. Y. Cho, "Impurity Profiles of GaAs Epitaxial Layers Doped with Sn, Si and Ge With Molecular Beam Epitaxy," J. Appl. Phys., 46, 1773, 1975.

10. H. Morkoç, A. Y. Cho and C. Radice, Jr., "Transport Properties of Sn-doped $Al_xGa_{1-x}As$ Grown by Molecular Beam Epitaxy," 51, 4882, 1980.

11. M. Illegems, "Beryllium Doping and Diffusion in Molecular Beam Epitaxy of GaAs and $Al_xGa_{1-x}As$," J. Appl. Phys., 48, 1278, 1977.

12. N. Duhamel, P. Henoc, F. Alexandre and E. V. K. Rao, "Influence of Growth Temperature on Be Incorporation in Molecular Beam Epitaxy GaAs Epilayers," Appl. Phys. Lett., 39, 49, 1981.

13. C. M. Stanchak, H. Morkoç, L. C. Witkowski and T. J. Drummond, "Automatic Shutter Controller for Molecular Beam Epitaxy," Rev. Sci. Instrum., 52, 438, 1981.

14. Ping-King Tien and J. A. Giordmaine, "Integrated Optics: Wave of the Future," Bell Lab. Rec., p. 371, 1980.

15. J. I. Pankove, "Optical Processes in Semiconductors," Dover Publications, Inc., p. 216, 1971.

16. J. C. Dyment, L. A. D'Asaro, J. C. North, B. I. Miller and J. E. Ripper, "Proton-Bombardment Formation of Stripe Geometry Heterostructure Lasers for 300 K CW Operation," Proc. IEEE, 60, 726, 1972.

17. R. W. Dixon and W. B. Joyce, "(Al,Ga)As Double-Heterostructure Lasers: Comparison of Devices Fabricated with Deep and Shallow Proton Bombardment," B. S. T. J., 59, 975, 1980.

18. H. C. Casey, Jr., A. Y. Cho and P. A. Barnes, "Application of Molecular Beam Epitaxial Layers to Heterostructure Lasers," IEEE J. Quant. Elect., QE-11, 467, 1975.

19. A. Y. Cho, Private communication, 1980.


DATE
ILME